Modeling the input and relaxation of vibrational energy in CO_2 plasmas

T. Silva[1], M. Grofulović[1], B.L. M. Klarenaar[2], O. Guaitella[3], R. Engeln[2] and V. Guerra[1],

[1]*Instituto de Plasmas e Fusão Nuclear, Instituto Superior Técnico, Universidade de Lisboa, Lisboa, Portugal*
[2]*Department of Applied Physics, Eindhoven University of Technology, 5600 MB Eindhoven, The Netherlands*
[3]*LPP, Ecole Polytechnique, UPMC, Université Paris Sud-11, CNRS, Palaiseau, France*

Abstract: This work contributes towards a detailed CO_2 kinetic scheme that describes the input and relaxation of vibrational energy in CO_2 plasmas. To this purpose, the vibrational energy exchanges in CO_2 discharges are investigated through a self-consistent model describing the time evolution of the population of individual vibrational levels of the $CO_2(X^1\Sigma^+)$. The model was validated by comparing the calculated densities of vibrationally-excited CO_2 molecules with experimental data obtained in a pulsed CO_2 glow discharge.

Keywords: CO_2 discharges, CO_2 dissociation, vibrational excitation, vibrational energy transfer.

1. Introduction

It is well known that the steadily rising atmospheric concentration of CO_2 over the past century is contributing to the greenhouse effect and planetary heating. As a response to these issues, there is an increasing interest for technologies that convert CO_2 into value-added chemicals, as they can effectively recycle waste into new feedstock [1-2]. In this context, and given the necessity to achieve an efficient CO_2 conversion, non-equilibrium plasma technologies have gained significant attention [3]. The great potential of plasma technology for CO_2 conversion is due to the presence of energetic electrons that enhance specific reaction channels which can lead to an efficient molecular decomposition. This is often associated with the well-known vibrational ladder-climbing mechanism, in which the CO_2 molecules are promoted to higher vibrational levels through inter-molecular collisions [4]. This subject has been extensively studied in the past years through different plasma experiments including coronas [5], radio frequency discharges [6], microwave discharges [7]. dielectric-barrier discharges [8] and gliding arc plasmatrons [9]. In what concerns modeling work, however, there is some lack of research involving a complete state-to-state model for the vibrational kinetics of CO_2 under non-equilibrium conditions. Recently, Kozák *et al.* [10] have developed a CO_2 kinetic reaction model with a very complete plasma chemistry, but they have considered only about 25 CO_2 vibrational levels. Another recent study has considered more than 9000 CO_2 vibrational levels, but does not include electron kinetics [11]. Despite the high relevance of these works, the disparity of formulations raises the question about the advantages and disadvantages of each approach.

In this contribution, we provide a comprehensive CO_2 kinetic scheme that describes the input and relaxation of vibrational energy in the lowest CO_2 vibrational levels under non-equilibrium conditions. To this purpose, we have solved the rate balance equation for the concentration of ~ 70 vibrational levels of CO_2. The paper is organized as follows: in Section 2, we review some relevant aspects of CO_2 vibrational kinetics which are of special importance in this work; in section 3, we describe our model, together with all the assumptions made; in section 4 we present the results obtained, as well as the comparison with experimental results; section 5 summarizes this work.

2. Vibrational kinetics in CO_2

The CO_2 molecule is a linear triatomic molecule, and as such it possesses three normal vibrational modes: the symmetric stretching, the double degenerate bending and the asymmetric stretching. These modes are characterized by the quantum numbers v_1, v_2, and v_3, respectively. The degenerated bending vibration consists of two component vibrations which result in a quasi-rotation of the linear molecule around its principal axis. In order to quantify this rotational motion, an additional quantum number l_2 is necessary. This quantum number can take the values: $l_2 = v_2, v_2 - 2, v_2 - 4,..1$ or 0, depending on whether v_2 is odd or even (more details can be found in Ref. [12]). A typical symbol for a particular vibrational level has the form $CO_2(v_1 v_2^{l_2} v_3)$ (also known as *Herzberg* notation [12]).

There is another special feature of CO_2 molecules worth mentioning: *the Fermi resonance*. Such a resonance happens because v_1 and $2v_2$ modes have close vibrational energies and the same type of symmetry. This interaction couples the levels CO_2 $(v_1 v_2^{l_2} v_3)$ to the levels CO_2 $((v_1 - 1)(v_2+2)^{l_2} v_3)$ to form two new states that are often assumed to be in local equilibrium. According to the notation used by Rothman *et al* [13] these states are differentiated by the ranking index, *r*, which is unity for the highest vibrational level of a Fermi resonating group. More specifically, the CO_2 vibrational levels can be written as $v_1 v_2\, l_2\, v_3\, r$, where the ranking index, *r* can assume the values $r = 1,2,..,v_1+1$.

In this work, the CO_2 vibrational levels under Fermi resonance are always grouped as one effective level. Therefore, the vibrational energy of this effective level is determined through the average of vibrational energies (using the anharmonic oscillator approximation [10]) of the

individual vibrational states, while its statistical weight is determined through the sum of the individual statistical weights. These effective levels are denoted in this work by the form $v_1v_2\ l_2\ v_3\ r$, where r is always taken as v_1+1 (see Table 1).

Table 1. Comparison of notations for vibrational energy states. In this work the levels coupled by Fermi resonance are always considered as one effective level (see text).

Herzberg [12] CO_2 ($v_1v_2^{l_2}v_3$)	*Rothman* [13] CO_2 ($v_1v_2\ l_2v_3r$)	*This work* CO_2 ($v_1v_2\ l_2v_3r$)
CO_2 (00^00)	CO_2 (00001)	CO_2 (00001)
CO_2 (01^10)	CO_2 (01101)	CO_2 (01101)
CO_2 (02^20)	CO_2 (02201)	CO_2 (02201)
CO_2 (10^00)	CO_2 (10001)	CO_2 (10002)
CO_2 (02^00)	CO_2 (10002)	
CO_2 (20^00)	CO_2 (20001)	CO_2 (20003)
CO_2 (12^00)	CO_2 (20002)	
CO_2 (04^00)	CO_2 (20003)	

3. Model description

In this work, we develop a kinetic scheme to describe the time-resolved densities of several CO_2 vibrational levels. More specifically, the rate balance equations for the creation and loss of the levels are investigated. The different processes to be taken into account include electron-vibration (e-V), vibration-vibration (V-V) and vibration-translation (V-T) exchanges (see Table 2). We have assumed a low excitation regime in which only a few vibrational levels are excited. At this stage, we have considered $v_2^{\max} = v_3^{\max} = 5$, which leads to a total of 72 CO_2 vibrational levels with a vibrational excitation up to about 2 eV. Note that these 72 vibrational levels include the effective levels as a result of the Fermi resonance (as discussed in the previous section). The concentration for each of these vibrational levels, n_v, can then be calculated from:

$$\frac{dn_v}{dt} = n_e \sum_{w\neq v} n_w C_w^v - n_e n_v \sum_{w\neq v} C_v^w - n_v[\mathrm{CO_2}]P_{v,v-1} + n_{v+1}[\mathrm{CO_2}]P_{v+1,v} + n_{v-1}[\mathrm{CO_2}]P_{v-1,v} - n_v[\mathrm{CO_2}]P_{v,v+1} - n_v \sum_w n_{w-1} Q_{v,v-1}^{w-1,w} + n_{v-1} \sum_w n_w Q_{v-1,v}^{w,w-1} + n_{v+1} \sum_w n_{w-1} Q_{v+1,v}^{w-1,w} - n_v \sum_w n_w Q_{v,v+1}^{w,w-1}, \quad (1)$$

where n_e and $[\mathrm{CO_2}]$ are the electron and molecular densities, respectively, C, P and Q denote the rate coefficients for e-V, V-T and V-V processes, respectively. The system (1) shows unambiguously the strong link between the different kinetics. First, electrons determine the energy input into the vibrational mode, expressed by the excitation coefficients C_w^v. This energy is redistributed among the vibrational manifold through V-V and V-T exchanges. A decisive step to obtain realistic populations of vibrationally excited molecules in different levels is the choice of the collisional data in equation (1). In this work the V-T and V-V rate coefficients between the lowest vibrational states are computed using the available rates in Blauer *et al.* [14] and Kreutz *et al.* [15], while the remaining rate coefficients (for higher states) are calculated on the basis of the SSH theory [16]. All rates involving V-T and V-V exchanges have been approximated by:

$$k\ (T_{gas}) = \mathrm{Exp}(A + B\ T_{gas}^{-1/3} + \mathrm{C}\ T_{gas}^{-2/3}), \quad (2)$$

where A, B, C are constants and T_{gas} is the gas temperature.

For the active part of the discharge involving e-V exchanges, the rate balance equation for the creation and loss of CO_2^+ ions is added to the system. The self-consistent sustaining electric field can then be calculated as described in [17]. The electron impact rate coefficients can also be obtained from the solution of the electron Boltzmann equation in the usual two-term expansion in spherical harmonics using the cross sections from [18]. When the electron-impact cross sections are not available, we calculate the remaining rate coefficients on the basis of the Fridman approximation [4].

For the reverse processes, i.e. reactions that result from the de-excitation of molecules, the rate coefficients are computed through detailed balance, assuming an electron temperature T_e for e-V exchanges, and T_{gas} for V-T and V-V exchanges, according to:

$$C_v^w = C_w^v \mathrm{Exp}\left(-\frac{\Delta E_w^v}{KT_e}\right), \quad (3)$$

$$P_{v-1,v} = P_{v,v-1} \mathrm{Exp}\left(-\frac{\Delta E_{v,v-1}}{KT_{gas}}\right), \quad (4)$$

$$Q_{v-1,v}^{w,w-1} = Q_{v,v-1}^{w-1,w} \mathrm{Exp}\left(-\frac{\Delta E_{v,v-1}^{w-1,w}}{KT_{gas}}\right), \quad (5)$$

where ΔE represents the energy difference between the relevant vibrational states. At the present stage, the model accounts (including direct and inverse processes) with 530, 1188 and 294 V-T, V-V and e-V reactions respectively.

Table 2. Kinetic processes considered in this work for the description of CO_2 vibrational states.

	Reaction
e-V	$e + CO_2(v) \leftrightarrow e + CO_2(w)$; *Example:* e+ CO_2 (00001) $\leftrightarrow$ $e + CO_2$ (00011)
V-T	$CO_2(v) + CO_2 \leftrightarrow CO_2(v-1) + CO_2$; *Example:* CO_2 (01101) + CO_2 $\leftrightarrow$ CO_2 (00001) + CO_2
V-V	$CO_2(v) + CO_2(w) \leftrightarrow CO_2(v-1) + CO_2(w+1)$; *Example:* CO_2 (00011) + CO_2 (00011) $\leftrightarrow$ CO_2 (00001) + CO_2 (00021)

4. Results

The solutions from the rate balance equation (1) are shown in this section. As initial values for the concentrations of the various vibrational states we have imposed two vibrational temperatures through Boltzmann distributions. More specifically, the changes in the v_3 mode relate to one vibrational temperature T_3, while the v_1 and

v_2 modes are assumed to be in equilibrium at the same vibrational temperature, i.e. $T_1 = T_2 = T_{12}$. Fig.1 shows a typical distribution of the CO_2 molecules among energy levels assuming T_3 =1500 K (determined by the slope of the solid lines) and T_{12} = 300 K (determined by the slope of the dashed lines).

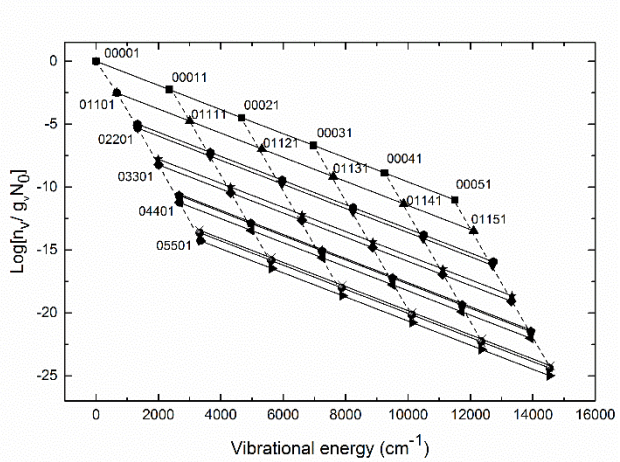

Fig.1. Boltzmann distributions of the CO_2 molecules with T_3 =1500 K and T_{12} = 300 K. Some of the CO_2 vibrational levels are indicated. N_0 and g_v represent the ground state density and statistical weigh of the level v.

4.1 – Limit case: only V-T and V-V exchanges

As a first step to verify our calculations, we have analyzed the solutions of (1) under the limit case which neglects all the electronic collisions. In other words, the first and second terms of (1) are omitted and only V-T and V-V exchanges are considered. In practice, this limit should approximate an afterglow regime where the electron temperature/density decays rapidly, resulting in drastic decrease in the rates involving electron impact collisions. This situation is illustrated in Fig. 2 where an equilibrium of vibrational temperatures (in our case represented by T_{12} and T_3) with the gas temperature can be observed after about 10^{-2} s.

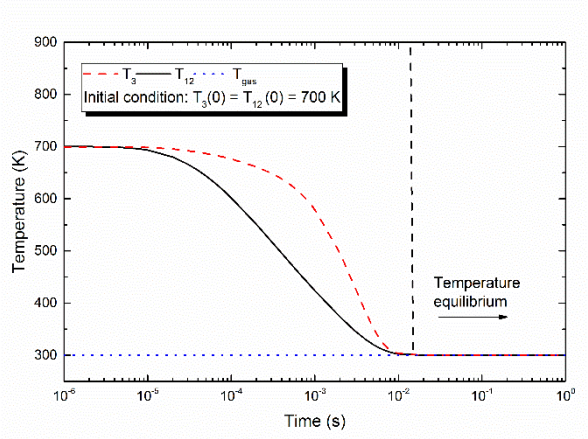

Fig.2. Vibrational temperatures calculated from the solution of the rate balance equations (1) in the absence of electronic collisions. T_{gas} = 300 K and pressure = 5 Torr.

4.2 – Comparison with the experiment

In order to validate our model, the calculated concentrations of the CO_2 vibrational levels were compared with the experimental densities (obtained via time-resolved in situ Fourier Transform Infrared spectroscopy) in a pulsed CO_2 glow discharge under low excitation conditions. The system under analysis operates with pressure p = 5 Torr, current I = 50 mA and a pulse width of 5 ms. For more details about the experimental setup, see [19].

In what concerns the model input, it is worth mentioning that the gas temperature profile, as well as the initial values of T_3 and T_{12} are always taken from the experimental data. Fig.3 shows the calculated and measured results relative to the density of the first excited CO_2 asymmetric state (i.e. $v_1 = v_2 = l_2 = 0$ and v_3 = 1) during the off-time of the discharge. Only V-V and V-T exchanges were considered in these calculations. As one can see, there is an excellent agreement between the calculated and experimentally determined densities.

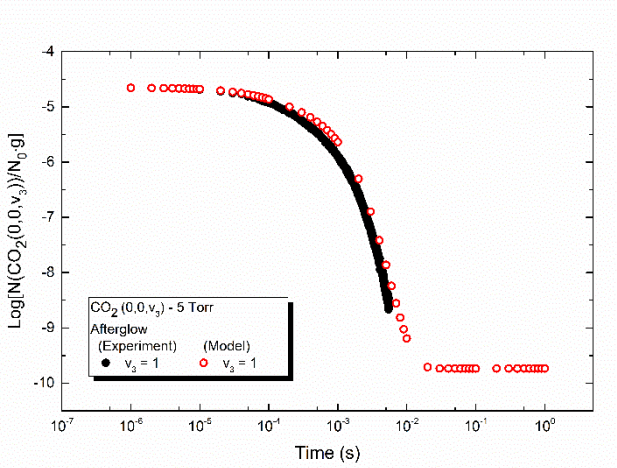

Fig.3 Normalized density of the first excited CO_2 asymmetric state during the afterglow of a pulsed DC discharge for p = 5 Torr and I = 50 mA. Open symbols represent the calculation results, while close symbols the experimental data.

For the active part of the discharge, we solve the system (1) with the complete set of e-V, V-V and V-T exchanges, as well as the rate balance equation for CO_2^+ ions. The electron density used in these calculations (~ 4.5 $\times 10^9$ cm^{-3}) is estimated based on the experimental current and the calculated electron drift velocity [18]. At the same time, the calculated maintenance reduced electric field is 63 Td, which is in excellent agreement with the experimental measurements. The actual comparison between calculated and measured results in the active part of the discharge is shown in Fig.4 for the first excited CO_2 asymmetric state.

As one can see, the calculated and measured densities have the similar trend during the on-time of the plasma pulse, which reinforces the validity of our CO_2 kinetic scheme.

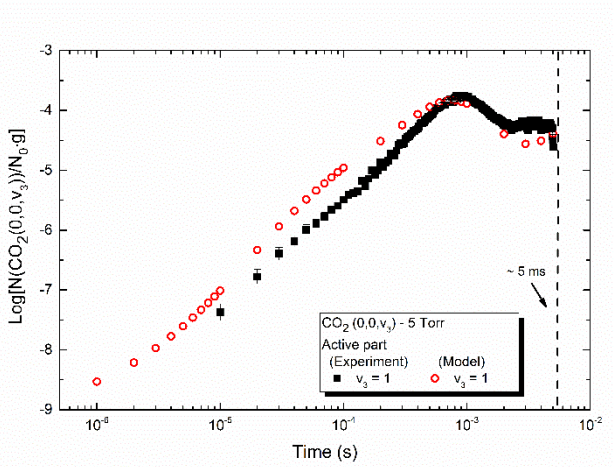

Fig.4. Normalized density of the first excited CO_2 asymmetric state during the active part of a pulsed DC discharge for p = 5 Torr and I = 50 mA. Open symbols represent the calculation results, while close symbols the experimental data.

5. Summary

In this work, we have developed a kinetic model that describes the input and relaxation of vibrational energy in CO_2 discharges. More specifically, we have investigated the rate balance equations for the manifold of several CO_2 vibrational levels including the processes of electron-vibration, vibration-vibration and vibration-translation energy exchanges. The model was validated from the comparison of the calculations with the experimental data obtained in a pulsed CO_2 glow discharge. The modeling work is in progress in order to: (i) extend our research to higher vibrational excitations up to the dissociation limit of CO_2 and (ii) include other species (CO, O, etc.) that play an important role in the chemistry of CO_2 discharges.

6. Acknowledgments

This work was partially supported by the Portuguese FCT, under Projects UID/FIS/50010/2013 and PTDC/FIS-PLA/1420/2014. VG and RE have been supported by LABEX Plas@par receiving financial aid managed by the Agence Nationale de la Recherche under the reference ANR-11-IDEX-0004-02.

7. References

[1] A. P. H. Goede, EPJ Web of Conferences, **98**, 07002 (2015).
[2] G. Centi, E. A. Qiadrelli and S. Perathoner, Energy & Environment Science, **6**, 1711 (2013).
[3] A. Bogaerts, T. Kozak, K. van Laer and R. Snoeckx, Faraday Discuss., **183**, 217-232 (2015).
[4] V.D. Rusanov, A.A. Fridman, G.V. Sholin, Usp. Fiz. Nauk, **134**, 6 (1981).
[5] A. M. Ghorbanzadechm, R. Lotfalipou, S. Reze, Int. J. Hydrog. Energy, **34**, 293 (2009).
[6] L. F. Spencer, A. D. Gallimore, Plasma Chem. Plasma Process. **31**, 79 (2011).
[7] T. Silva, N. Britun, T. Godfroid, R. Snyders, Plasma Sources Sci. Technol. **23**, 025009 (2014).
[8] A. Ozkan, T. Dufour, T. Silva, N. Britun, R. Snyders, A. Bogaerts, F. Reniers, Plasma Sources Sci. Technol. **25**, 025013 (2016).
[9] T. Nunnally, K. Gutsol, A. Rabinovich, A. Fridman, A. Gutsol, A. Kemoun, J. Phys. D: Appl. Phys. **44**, 274009, (2011).
[10] T. Kozák, A. Bogaerts, Plasma Sources Sci. Technol. **23**, 0450 (2014).
[11] I. Armenise, E. V. Kustova, Chemical Physics **45**, 269-281 (2013).
[12] G. Herzberg, Infrared and Raman spectra of polyatomic molecules, Van Nostrand, New York, 1951.
[13] L. S. Rothman and L. D. G. Young, J. Quant. Spectrosc. Radiat. Transfer. **25**, 505-524 (1981).
[14] J. A. Blauer and G. R. Nickerson, Rep. Ultrasystems Inc. (1973).
[15] T. G. Kreutz, J. A. O'Neill and G. W. Flynn, J. Phys. Chem. **91**, 5540 (1987).
[16] R. N. Shwartz, Z. I. Slawsky and K. F. Herzberg, J. Chem. Phys. **20**, 1591 (1952).
[17] C. D. Pintassilgo, V. Guerra, O. Guaitella and A. Rousseau, Plasma Sources Sci. Technol. **23**, 0255006 (2014).
[18] M. Grofulović, L. L. Alves and V. Guerra, J. Phys. D: Appl. Phys. **49**, 395207 (2016).
[19] B.L.M. Klarenaar, R. Engeln, M.A. Damen, M.C.M. van de Sanden, A.S. Morillo-Candas, P. Auvray, and O. Guaitella, contribution submitted to ISPC 23, (2017).